Orbicular gabbro from near Baskil, southeastern Turkey

EVREN YAZGAN AND ROGER MASON

Department of Geological Sciences, University College, Gower Street, London WC1E 6BT

Abstract

The first occurrence of orbicular rocks in Turkey is reported. They are gabbros in a dyke in the Baskil island-arc magmatic suite, of the southern branch of the Alpine–Himalayan chain. The orbicules have lithologically varied cores, regular shells of troctolitic composition, with a radial arrangement of olivine and plagioclase crystals, and a matrix of vari-textured gabbro. Rock and mineral analyses indicate that magmatic crystallization began near the inner margin of the troctolitic shells. Metamorphic hydration of minerals in cores, shells and matrix followed directly after the later stages of magmatic crystallization, as part of a continuous process, and thus a magmatic–metamorphic origin for the orbicules is proposed. Alternative hypotheses for the development of the orbicules are discussed: one involving the development of a protocrystalline magma shell, the other rapid crystallization during upward migration of xenolith-bearing magma.

KEYWORDS: orbicules, gabbro, Turkey.

Introduction

ORBICULAR rocks are very rare and interesting, notably for their peculiar mineralogical texture, which has attracted the attention of geologists for many years. Some of the best known examples are the orbicular diorite of Santa Lucia-di-Tallano, Corsica (Maisonneuve, 1960), the orbicular granites of Finland (Frosterus, 1892, 1896; Sederholm, 1928; Eskola, 1938; Simonen, 1941; 1966; Perttunen, 1983), the orbicular granodiorite of Antarctica (Palmer et al., 1967) and the orbicular rocks of Montana and Wyoming, U.S.A. (Leveson, 1963).

Yazgan has discovered the first orbicular rocks in Turkey. They are of the most rare orbicular rock-type, gabbro, of which only about eight other occurrences have been recorded (Lawson, 1902; Watson, 1904; Campbell, 1906; Schaller, 1911; Satterly, 1940; Carstens, 1957; Merriam, 1958; Barrière, 1972; Lee and Sharpe, 1979; Van Diver and Maggetti, 1975; and Maggetti et al., 1978). The orbicular structures are found in a single dyke intrusion in the Baskil Magmatic Suite at 38°55′E, 38°37′N, 9 km northeast of Baskil and approximately 35 km west of Elazig, in southern Turkey (Fig. 1). The dyke is lenticular in shape, approximately 20 m long, and reaching a maximum thickness of 3–4 m. It is elongated parallel to the NE–SW strike of the Taurus orogenic belt of southern Turkey in this district.

Field relationships

The Baskil Magmatic Suite formed as part of a magmatic arc existing in Coniacian to Santonian times, during the complex evolution of the Taurus orogenic belt. Plutonic members of the suite have given radiometric ages in the range 84–86 Ma (Yazgan, 1983; Yazgan et al., 1983). The dyke is found in the zone of hornfelses and skarns surrounding a larger tonalitic mass, which is not orbicular. The contact metamorphic rocks were formerly pyroclastic rocks and hypabyssal intrusives, and now contain such mineral assemblages as augite + hypersthene + magnesio-hornblende + plagioclase (An_{43}) + quartz + magnetite and hedenbergite + andradite + plagioclase (An_{92}) + sphene + magnetitie + quartz. There are hornblende hornfels facies contact rocks and greenschist facies assemblages further away from the tonalite contact.

The contacts of the orbicular gabbro with the country rocks are sharp, and show no comb layering (cf. Moore and Lockwood, 1973). Comb layering is, however, seen in an intrusion of granite of the Baskil magmatic suite into pyroxenite and peridotite country rocks at a deeper structural level in the former island arc complex. All the orbicules occurring in the dyke are complete and

LEGEND

Sedimentary Cover

Quaternary sediments

Middle Palaeocene and younger sedimentary rocks

Late Campanian-lower Maastrichtian syn-orogenic flysch

Late Cretaceous (Coniacian-Santonian) Baskil Magmatic Complex

Calc-alkaline volcanics and high-level intrusive rocks (dykes etc.)

Tonalite

Monzonite (monzodiorite)

Diorite

Gabbro

Palaeozoic Basement (Pre-intrusive)

Keban metamorphic rocks

Metamorphic rocks with skarns at contact with magmatic rocks
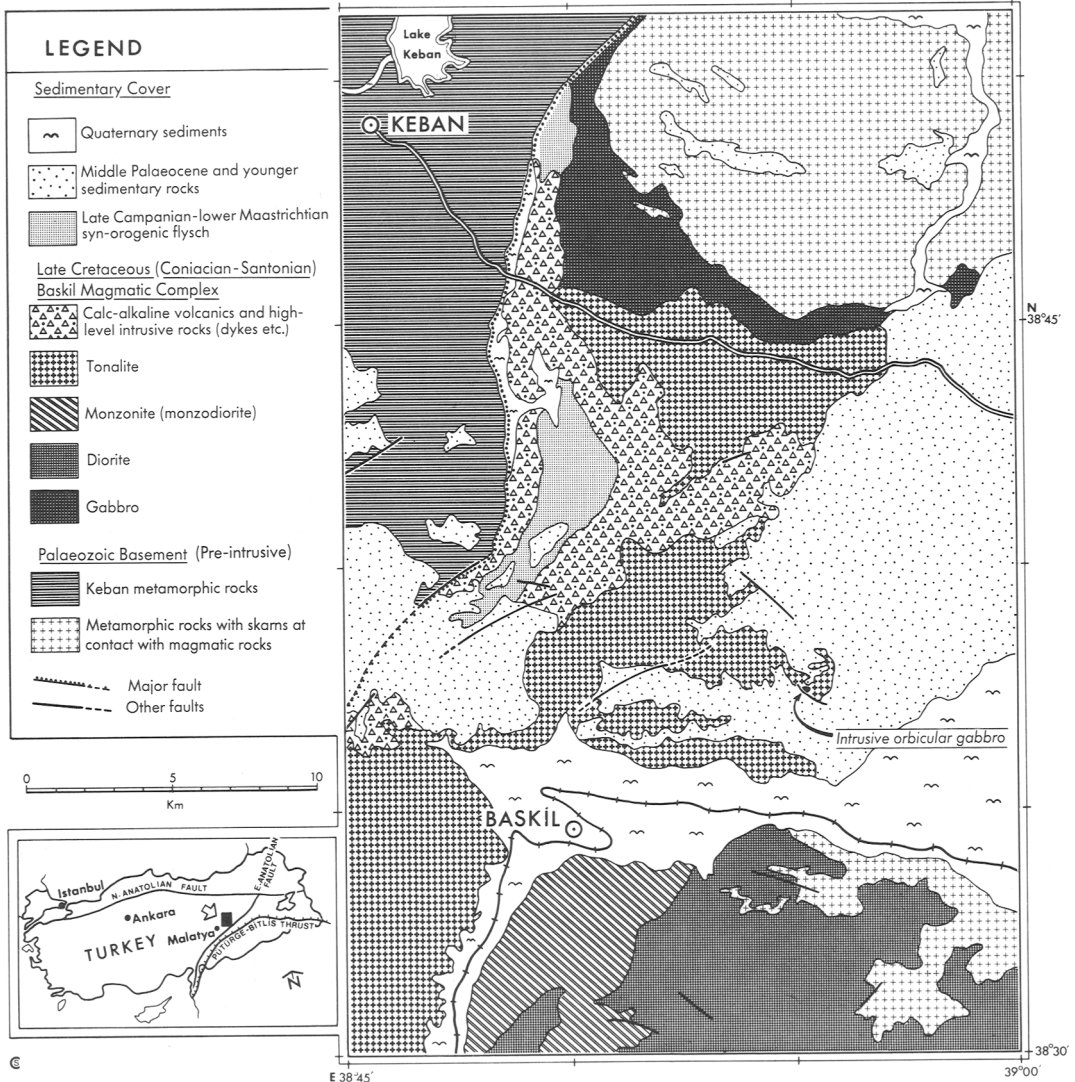
Major fault

Other faults

FIG. 1. Geological map of the Baskil region, SE Turkey, showing the location of the Baskil arc magmatic rocks and the orbicular gabbro, based upon unpublished maps by E. Yazgan and J. Asutay.

unbroken, and there are no xenoliths which are not orbicular. The orbicular dyke was intruded during a static phase in the tectonic evolution of the Taurus fold-belt, and shows no sign of deformation during or after intrusion.

The orbicules

The orbicules are generally spherical or ellipsoidal in form, but there are occasional rectangular shapes also (Fig. 2, cf. Augustithis, 1982; Leveson, 1966). They vary in diameter from 2 cm to 15 cm.

The orbicular gabbro may be divided into three different parts: (1) the cores of the orbicules; (2) a shell of troctolite with olivine and plagioclase crystals in a radial arrangement; and (3) the gabbroic matrix surrounding the orbicules. There is considerable variation between different orbicules, but the troctolitic shell (2) is always present and complete. The cores are particularly hetero-
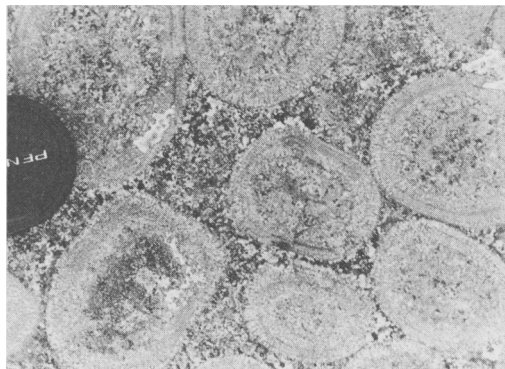
FIG. 2. Outcrop photograph of the orbicular gabbro. Note the angular outline of the orbicule core at lower left, and the variable texture of the matrix.

geneous.

Samples of core material, troctolitic shell and matrix were separated from one another by sawing apart, dissolved in HF and $HClO_4$, and the solutions analysed by I.C.P. in the Department of Geology, Royal Holloway and Bedford New College, London, by Dr J. N. Walsh. SiO_2 was determined separately by Atomic Absorption, and H_2O and CO_2 determined by thermal decomposition. The latter determinations and the preparation of the solutions for I.C.P. were carried out in the Department of Geological Sciences, University College, London, by A. T. Osborn. The results of the analyses are presented in Table 1.

The primary rocks of cores, troctolitic shells and matrix have undergone local retrograde hydrothermal metamorphism. The term 'metamorphism' is being used here to mean alteration in the solid state, often including the introduction of H_2O into anhydrous minerals, below the solidus temperatures of gabbroic melts. The authors do not imply by the use of the term that there was either an influx of heat or fluid into the cooling orbicular gabbro.

Cores. Three primary rock types have been recognized in the cores. They are: (A) aggregates of hornblende crystals; (B) olivine–plagioclase rocks (troctolites) with hornfelsic textures; and (C) olivine–hornblende gabbro, with magmatic crystallisation textures. Some orbicules have cores entirely composed of gabbro; others have either a combination of hornblende aggregate and gabbro, or a combination of hornfelsic troctolite and gabbro. Orbicules with two primary rocktypes in their cores may show a concentrically layered structure, with either an inner core of

hornblende aggregate, and an outer core of gabbro (Fig. 3), or an inner core of hornfelsic troctolite and an outer core of gabbro.

The gabbro contains anorthite plagioclase (An_{94}), olivine (Fo_{80}), orthopyroxene (En_{81}), clinopyroxene and hornblende. Two analyses are given in Table 1. The clinopyroxene has been partly replaced by the hornblende, which also crystallized magmatically, implying that the replacement was due to reaction of clinopyroxene with magma during the later stages of crystallization. Selected magmatic amphibole analyses are presented in Table 2: they are edenitic and pargasitic hornblendes. Unless otherwise stated, all analyses reported in this paper were conducted on the Cambridge Instruments Microscan V electron-probe in the Department of Geological Sciences, UCL, using an EDS method.

The primary core rocks have undergone hydrothermal metamorphism. Gabbro has been replaced by secondary plagioclase, zoisite, magnesian chlorite, actinolite and, locally, talc and spinel. The calcic amphiboles display a distinct compositional gap between the primary magmatic amphiboles and the secondary metamorphic amphiboles (Fig. 4). The local development of chessboard twinning patterns in the plagioclase of the gabbro appears to be due to the early stages of this metamorphism. The amphibole aggregates have altered to magnesian chlorite and actinolite. Analyses of amphiboles from the cores are presented in Table 2. In some orbicules (e.g. Fig. 3) the metamorphism has occurred in a concentric layer on both sides of the interface between the inner and the outer core. In general, this metamorphism is patchily distributed, and metamorphic zonation on a small scale is frequently a feature, apparently controlled by gradients in activity of H_2O during metamorphism.

The troctolitic shell is the most consistent and distinct feature of the orbicules. It is 13–20 mm thick, with uniform thickness round each individual orbicule. It consists of radiating prismatic crystals of olivine (Fo_{81}) and plagioclase (An_{91}). There are two or more concentric layers composed entirely of olivine within the shell, and a similar layer marks its outer limit. The inner limit passes gradationally into core gabbro, where the olivine and plagioclase crystals cease to have a radial structure (Figs 3 and 5). In some orbicules the troctolitic shell has been deformed where the orbicule has pressed against a neighbouring orbicule, apparently when the matrix was fluid and the core gabbro was plastic or fluid (Fig. 6).

In each layer of the shell, single olivine crystals run right across the layer, elongated approxima-

TABLE 1.

Analyses of core, troctolitic shell and matrix of a single orbicule.

	Core			Shell			Matrix	
	1	2	3	1	2	3	1	2
SiO_2	42.60	43.40	43.11	39.72	39.97	40.56	45.50	46.48
TiO_2	0.16	0.21	0.19	0.05	0.04	0.04	0.67	0.44
Al_2O_3	17.73	18.17	17.66	20.61	18.77	19.00	17.16	14.93
FeO*	8.13	8.39	8.05	8.14	9.27	9.21	9.60	11.09
MnO	0.14	0.18	0.16	0.15	0.16	0.16	0.18	0.22
MgO	15.96	14.18	15.19	15.18	17.69	17.39	10.53	13.89
CaO	9.84	9.95	10.20	10.95	9.77	9.79	10.32	8.42
Na_2O	0.64	0.84	0.93	0.64	0.62	0.62	2.47	1.58
K_2O	0.04	0.06	0.06	0.04	0.02	0.02	0.06	0.04
P_2O_5	0.05	0.05	0.06	0.05	0.05	0.04	0.11	0.07
H_2O+	3.61	3.07	3.21	2.74	2.33	2.36	1.84	1.18
H_2O-	0.40	0.62	0.53	0.42	0.58	0.44	0.41	0.33
CO_2	0.37	0.23	<0.05	0.18	0.16	0.20	0.37	<0.05
Total	99.67	99.35	99.35	98.87	99.43	99.83	99.22	98.67

FeO* - total Fe as FeO.

Analyses performed by ICP at Bedford Royal Holloway New College, London, by Dr J.N. Walsh. (Trace element analyses for Ba, Ce,Co, Cr, Cu, La, Li, Nb, Ni, Sc, Sr, V, Y, Zn available from the authors on request).

TABLE 2(a) Energy-dispersive microprobe analyses of pyroxenes: (G) core gabbro magmatic minerals.

Pyroxenes	G	G	G	G
SiO_2	54.50	54.16	54.92	55.35
Al_2O_3	2.06	2.16	1.31	1.88
TiO_2	0.27	0.00	0.00	0.15
Fe_2O_3	1.57	0.55	0.27	3.57
FeO	11.18	11.66	11.60	8.65
MnO	0.28	0.37	0.34	0.29
MgO	29.10	29.24	29.65	30.13
CaO	1.09	0.48	0.69	0.85
Na_2O	0.15	0.00	0.00	0.56
Total	100.20	98.63	98.78	101.43

Formulae calculated on the basis of 6 oxygens (Fe^{3+} calculated for 4 cations)

Si	1.934	1.947	1.969	1.930
Aliv	0.066	0.053	0.031	0.070
Alvi	0.020	0.038	0.024	0.007
Ti	0.007	0.000	0.000	0.004
Fe3	0.042	0.015	0.007	0.094
Fe2	0.332	0.351	0.348	0.252
Mn	0.008	0.011	0.010	0.009
Mg	1.539	1.566	1.584	1.565
Ca	0.041	0.018	0.027	0.032
Na	0.010	0.000	0.000	0.038
En	0.80	0.80	0.80	0.84
Ofs	0.18	0.19	0.18	0.14
Wo	0.02	0.01	0.01	0.02

tely parallel to their *y* crystallographic directions. The plagioclase crystals display a similar elongate habit, and show a distinctive 'arrow head' pattern of lamellar twinning (Fig. 7). Pyroxene is entirely absent from the shell, except where the latter has been cut by fractures which formed after the crystallization of the olivine and plagioclase (Fig. 3). Most of the fractures contain orthopyroxene which formed pseudomorphously after the olivine of the radial troctolite. This reaction has apparently released MgO into the escaping hydrous fluid, and this has precipitated as spinel along the fringes of the fracture (Fig. 8, cf. Mason, 1978, p. 220). The appearance of primary orthopyroxene in both the core gabbro and the matrix, defines the boundaries of the shell.

The radiating olivine and plagioclase crystals were analysed at close intervals along their lengths to see whether there is a systematic compositional change along them. A variation was detected, close to the limit of accuracy of EDS analysis. Further analyses were therefore performed by wavelength dispersion, for Fe and Mg in olivine, and for Ca and Si in plagioclase. The results are displayed in Fig. 9. There is a small but real varia-

tion in the composition of both minerals, showing a complex pattern of chemical zonation in relation to the structure of the radial shell. The significance of this feature will be discussed in the section on the mode of origin of the orbicules.

Metamorphism is not as marked in the shells as in the cores and matrix. The fractures filled by metamorphic orthopyroxene have been mentioned. There is also alteration of olivine to talc, particularly common adjacent to the matrix.

The matrix is heterogeneous, mostly composed of ophitic gabbro, with patches of gabbro pegmatite rich in magmatic hornblende, and of leucocratic plagioclase-rich material. The grain-size is very variable, like the vari-textured gabbros found at the high level in ophiolite complexes (Coleman, 1977). It consists of calcic plagioclase (An_{87}), orthopyroxene (En_{73}), olivine, clinopyroxene and magmatic hornblende (analyses in Table 3). The proportions of these minerals are variable, and in some places the matrix consists only of plagioclase and magmatic hornblende. The clinopyroxene is present in a small proportion, and shows magmatic alteration to hornblende, as in the core gabbro.

TABLE 2(b). Microprobe analyses of amphiboles from orbicule cores: (A) amphiboles from aggregate clusters; (G) core gabbro magmatic minerals; (M) secondary metamorphic amphiboles of core.

Amphiboles

	A	A	A	A	A	A	A	A	A	A	A	M	M	M	G	G
SiO$_2$	56.26	45.50	45.33	45.30	46.21	46.16	44.99	46.09	45.20	45.82	45.91	44.97	44.90	44.60	45.27	43.97
Al$_2$O$_3$	0.75	11.15	11.86	11.50	11.64	10.65	12.38	11.38	10.52	11.74	12.86	11.58	12.95	11.01	11.33	12.62
TiO$_2$	0.00	2.40	1.08	0.27	2.35	1.83	0.82	1.28	1.61	0.32	0.60	2.73	0.00	1.69	0.27	0.79
Cr$_2$O$_3$	0.00	0.00	0.00	0.19	0.00	0.00	0.22	0.00	0.00	0.00	0.18	0.17	0.19	0.00	0.00	0.30
Fe$_2$O$_3$	3.67	7.11	8.31	9.39	7.79	6.53	9.86	9.18	7.55	8.88	9.09	4.75	8.68	9.15	9.57	9.02
FeO	0.00	2.18	1.35	0.58	1.56	3.22	0.28	0.85	2.07	1.18	1.20	4.67	0.00	0.55	0.16	0.12
MnO	0.15	0.16	0.18	0.00	0.26	0.22	0.22	0.24	0.00	0.18	0.18	0.16	0.20	0.00	0.00	0.00
MgO	22.19	16.61	16.27	16.55	16.89	16.45	16.42	17.03	16.58	16.85	16.83	15.52	16.95	16.39	16.66	16.21
CaO	12.54	11.76	11.59	11.55	11.75	11.83	11.54	11.58	11.38	11.73	11.89	12.02	10.70	11.05	11.31	11.31
Na$_2$O	0.00	1.87	1.90	1.74	2.03	1.97	2.00	2.04	2.13	2.08	2.52	1.66	2.13	1.88	1.92	1.95
K$_2$O	0.00	0.31	0.28	0.59	0.28	0.35	0.48	0.47	0.38	0.79	0.41	0.38	0.00	0.38	0.41	0.42
Total	95.56	99.05	98.15	97.66	100.76	99.21	99.23	99.90	97.43	99.57	101.66	98.64	96.51	96.70	96.90	96.71

Formulae calculated on the basis of 23 oxygens

Fe3$^+$ calculated for 13 cations

	A	A	A	A	A	A	A	A	A	A	A	M	M	M	G	G
Si	7.860	6.394	6.412	6.441	6.373	6.494	6.309	6.410	6.461	6.416	6.300	6.384	6.396	6.398	6.468	6.300
Aliv	0.124	1.606	1.588	1.559	1.627	1.506	1.691	1.590	1.539	1.584	1.700	1.616	1.604	1.602	1.532	1.700
Alvi	0.000	0.241	0.389	0.369	0.266	0.260	0.356	0.276	0.234	0.354	0.380	0.322	0.571	0.260	0.376	0.432
Ti	0.000	0.254	0.115	0.029	0.244	0.194	0.086	0.134	0.173	0.034	0.062	0.291	0.000	0.182	0.029	0.085
Cr	0.000	0.000	0.000	0.021	0.000	0.000	0.024	0.000	0.000	0.000	0.018	0.021	0.021	0.000	0.000	0.034
Fe3	0.386	0.752	0.885	1.005	0.809	0.692	1.040	0.960	0.812	0.936	0.939	0.508	0.930	0.988	1.029	0.973
Fe2	0.000	0.256	0.160	0.069	0.180	0.379	0.033	0.099	0.248	0.138	0.138	0.555	0.000	0.066	0.019	0.015
Mn	0.018	0.019	0.022	0.000	0.030	0.026	0.029	0.000	0.000	0.021	0.021	0.019	0.024	0.000	0.000	0.000
Mg	4.620	3.478	3.430	3.507	3.472	3.449	3.432	3.530	3 532	3.517	3.442	3.283	3.598	3.504	3.547	3.461
Ca	1.877	1.771	1.757	1.760	1.736	1.783	1.734	1.726	1.743	1.760	1.748	1.828	1.633	1.699	1.731	1.736
Na	0.000	0.509	0.521	0.480	0.543	0.537	0.544	0.550	0.590	0.565	0.670	0.457	0.588	0.523	0.532	0.542
K	0.000	0.056	0.051	0.107	0.049	0.063	0.086	0.083	0.069	0.141	0.072	0.069	0.000	0.070	0.075	0.077
Sum Tet	7.984	8.000	8.000	8.000	8.000	8.000	8.000	8.000	8.000	8.000	8.000	8.000	8.000	8.000	8.000	8.000
M1-M3	5.024	5.000	5.000	5.000	5.000	5.000	5.000	5.000	5.000	5.000	5.000	5.000	5.124	5.000	5.000	5.000
M4	1.877	2.000	2.000	2.000	2.000	2.000	2.000	2.000	2.000	2.000	2.000	2.000	2.000	2.000	2.000	2.000
A	0.000	0.336	0.328	0.346	0.329	0.384	0.364	0.359	0.403	0.466	0.491	0.354	0.222	0.291	0.338	0.355

Amphiboles

	G	G	G	G	G	G	G	G	M	M	M	M	M	M	M	M
SiO$_2$	45.61	43.95	43.55	44.03	44.26	44.90	43.88	42.75	49.14	48.46	47.34	50.17	49.57	48.07	45.28	45.99
Al$_2$O$_3$	13.29	12.35	11.60	12.19	12.90	11.68	11.31	12.04	9.73	8.91	10.69	9.55	8.30	10.61	11.78	11.27
TiO$_2$	0.00	0.64	2.30	0.69	0.50	1.58	2.76	3.52	0.00	0.45	0.00	0.00	0.00	0.00	0.59	0.58
Cr$_2$O$_3$	0.00	0.00	0.00	0.00	0.23	0.00	0.00	0.00	0.00	0.00	0.00	0.00	0.00	0.00	0.00	0.00
Fe$_2$O$_3$	8.45	8.38	7.67	8.73	9.65	8.83	8.80	5.99	7.38	8.85	9.56	5.37	7.20	9.14	9.17	7.95
FeO	0.00	1.31	1.77	1.01	0.00	0.92	1.62	4.08	0.00	0.00	0.00	1.56	0.67	0.00	0.00	0.39
MnO	0.00	0.17	0.00	0.00	0.00	0.18	0.15	0.00	0.31	0.23	0.00	0.00	0.18	0.00	0.18	0.00
MgO	17.10	15.91	15.88	16.10	16.23	16.80	16.22	15.15	19.36	20.06	16.90	18.22	18.26	17.60	17.06	17.07
CaO	11.36	11.51	11.00	11.22	11.04	11.39	11.07	11.13	11.07	9.18	11.20	12.16	11.79	11.42	11.41	11.53
Na$_2$O	2.30	2.03	2.20	2.20	2.30	2.48	2.54	2.53	1.16	1.22	1.39	1.36	1.55	1.94	1.90	1.86
K$_2$O	0.00	0.40	0.33	0.48	0.44	0.35	0.28	0.27	0.00	0.11	0.00	0.13	0.00	0.00	0.30	0.21
Total	98.11	96.65	96.30	96.64	97.55	99.11	98.63	97.46	98.15	97.47	97.08	98.52	97.52	98.78	97.67	96.85

Formulae calculated on the basis of 23 oxygens

Fe3$^+$ calculated for 13 cations

|	G	G	G	G	G	G	G	G	M	M	M	M	M	M	M	M
Si	6.391	6.331	6.299	6.337	6.293	6.313	6.230	6.169	6.812	6.775	6.684	6.944	6.952	6.678	6.410	6.537
Aliv	1.609	1.669	1.701	1.663	1.707	1.687	1.770	1.831	1.188	1.225	1.316	1.056	1.048	1.322	1.590	1.463
Alvi	0.586	0.428	0.278	0.405	0.455	0.248	0.123	0.217	0.402	0.243	0.463	0.502	0.324	0.416	0.376	0.426
Ti	0.000	0.069	0.250	0.075	0.053	0.167	0.295	0.382	0.000	0.047	0.000	0.000	0.000	0.000	0.063	0.062
Cr	0.000	0.000	0.000	0.000	0.026	0.000	0.000	0.000	0.000	0.000	0.000	0.000	0.000	0.000	0.000	0.000
Fe3	0.891	0.909	0.835	0.945	1.032	0.934	0.940	0.651	0.770	0.931	1.015	0.559	0.760	0.955	0.977	0.850
Fe2	0.000	0.157	0.214	0.121	0.000	0.109	0.192	0.492	0.000	0.000	0.000	0.180	0.078	0.000	0.000	0.046
Mn	0.000	0.021	0.000	0.000	0.000	0.021	0.018	0.000	0.036	0.027	0.000	0.000	0.021	0.000	0.022	0.000
Mg	3.571	3.416	3.423	3.453	3.439	3.520	3.432	3.258	4.000	4.179	3.556	3.758	3.816	3.644	3.599	3.616
Ca	1.706	1.777	1.705	1.730	1.682	1.716	1.684	1.721	1.644	1.375	1.694	1.803	1.772	1.700	1.731	1.756
Na	0.625	0.567	0.617	0.614	0.634	0.676	0.699	0.708	0.312	0.331	0.381	0.365	0.421	0.523	0.522	0.513
K	0.000	0.074	0.061	0.088	0.080	0.063	0.051	0.050	0.000	0.020	0.000	0.023	0.000	0.000	0.054	0.038
Sum Tet	8.000	8.000	8.000	8.000	8.000	8.000	8.000	8.000	8.000	8.000	8.000	8.000	8.000	8.000	8.000	8.000
M1-M3	5.048	5.000	5.000	5.000	5.005	5.000	5.000	5.000	5.208	5.428	5.034	5.000	5.000	5.015	5.037	5.000
M4	2.000	2.000	2.000	2.000	2.000	2.000	2.000	2.000	1.956	1.706	2.000	2.000	2.000	2.000	2.000	2.000
A	0.330	0.417	0.383	0.432	0.396	0.455	0.434	0.478	0.000	0.000	0.075	0.191	0.193	0.222	0.307	0.307
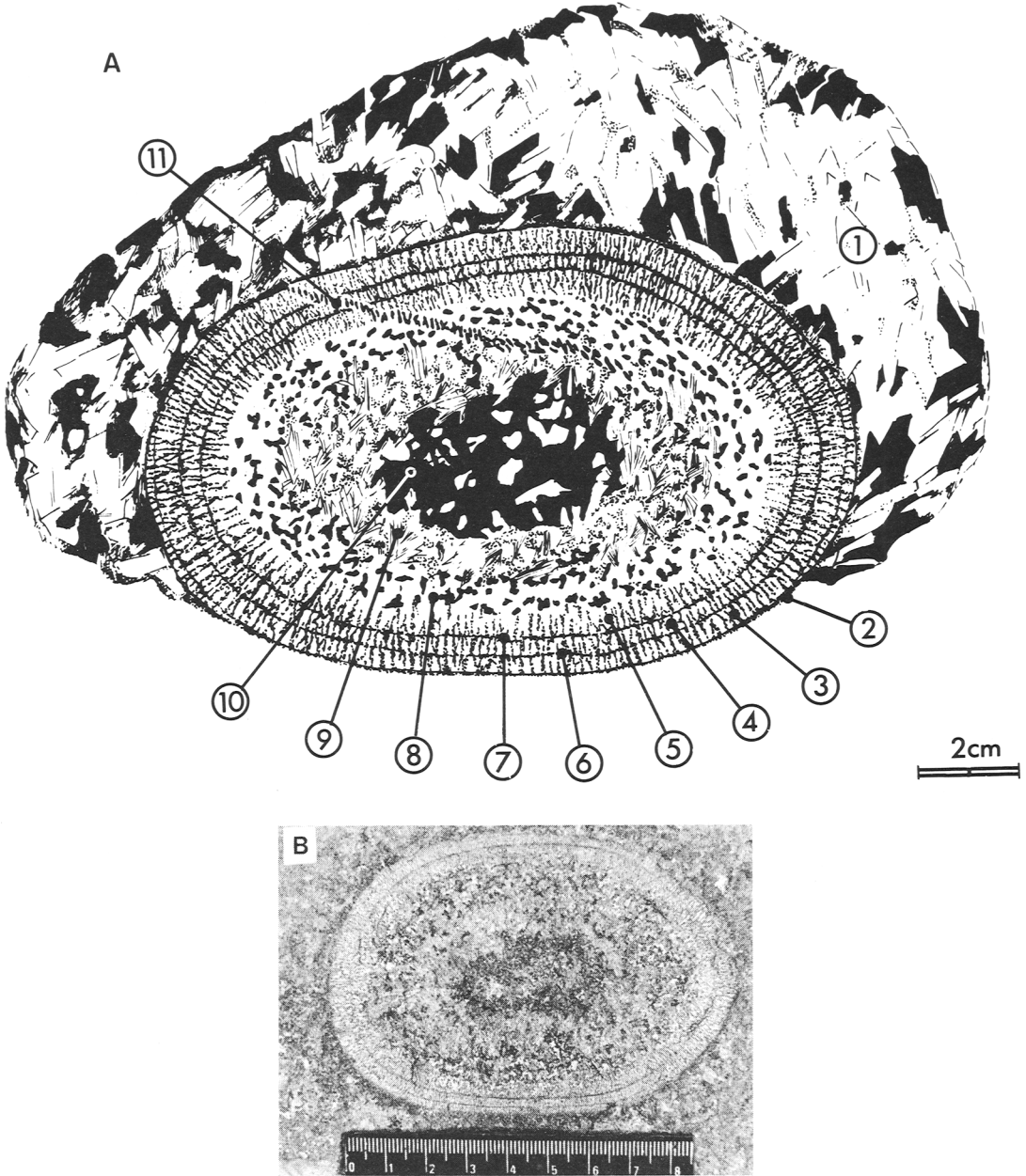
FIG. 3. Structure of an individual orbicule. (A) Sketch of parts of an orbicule: (1) matrix; (2) sharply defined outer limit of troctolitic shell; (3) outer layer of troctolitic shell; (4) middle layer of troctolitic shell; (5) inner layer of troctolitic shell; (6) and (7) layers of olivine separating troctolitic layers of shell; (8) core gabbro; (9) metamorphosed core material; (10) amphibole aggregates in core; (11) vein cutting through core and troctolitic shell. (B) Photograph of individual orbicule showing all the features indicated in Fig. 3A. Scale in centimetres.
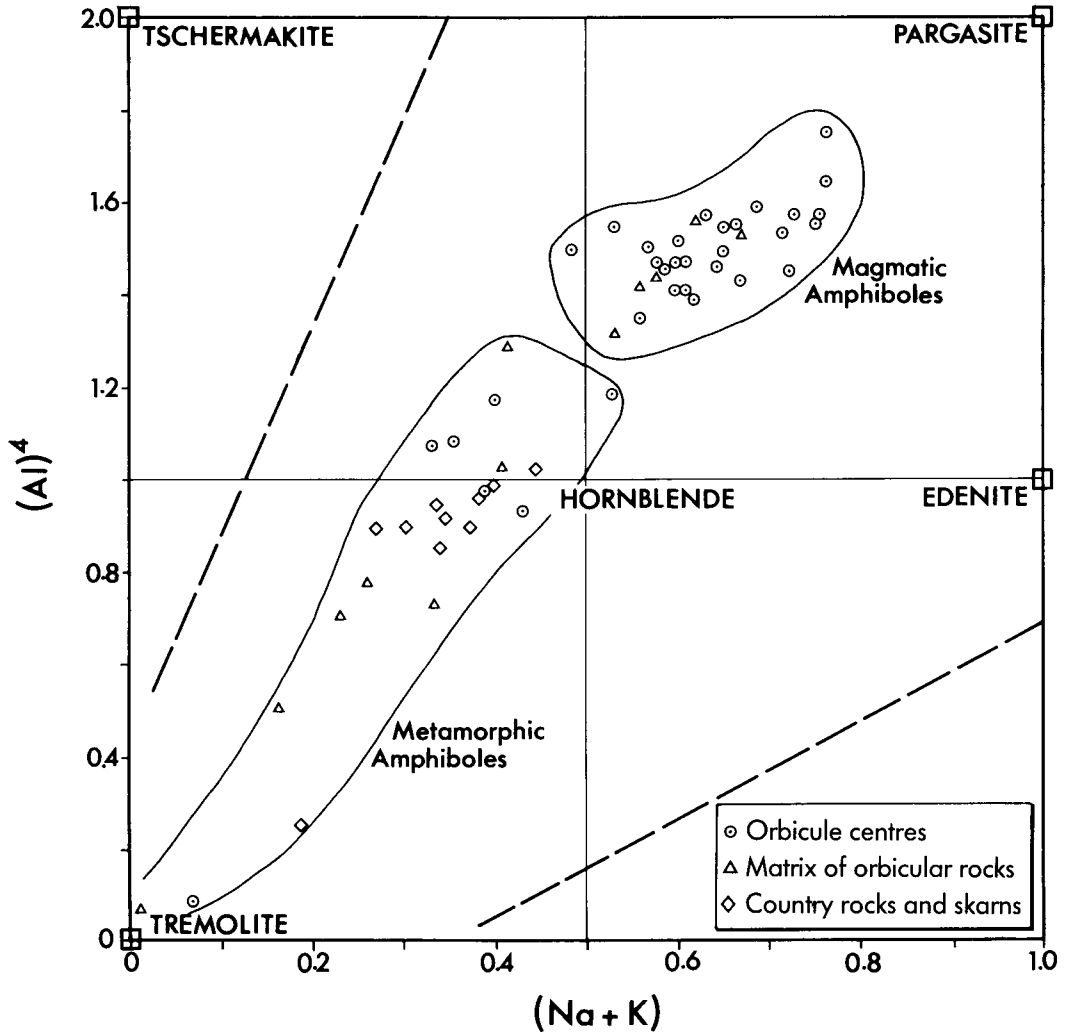
FIG. 4. Compositions of amphiboles from the orbicular gabbro and its country rocks, plotted on a $(Na + K)$ against Al^{iv} diagram. Fields of magmatic amphiboles and metamorphic amphiboles, distinguished by textural study, are indicated.

Local metamorphism has occurred in the matrix, giving rise to actinolite and actinolitic hornblende, and recrystallization of plagioclase. Some of the metamorphic amphibole has formed from primary magmatic amphibole. Analyses are given in Table 3.

Mode of origin of the orbicules

Features of the orbicular gabbro which the authors would emphasize for consideration in hypotheses for the origin of orbicular rocks in general are: (1) the magmatic arc setting of the Baskil igneous complex; (2) the hypabyssal nature of the orbicular gabbro dyke; (3) the hydrous character of both core and matrix gabbros; (4) the heterogeneous character of the core lithologies, especially the presence of the ultrabasic amphibole aggregates; (5) the chemical zonation of olivine in the troctolitic shells, which indicates that crystallization began at the shell/core interface.

The sequence of events involved in the formation of the orbicules is illustrated in Fig. 10 as follows:

(a) Basaltic magma was introduced into pyroxenite and amphibolite country-rocks at a deeper structural level in the Baskil magmatic arc than
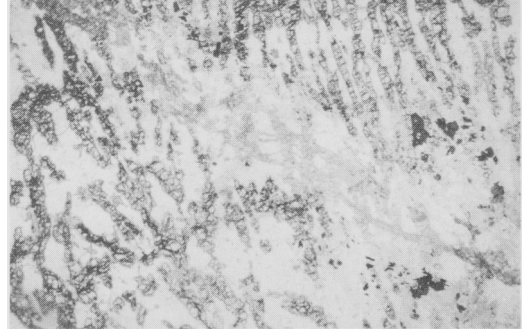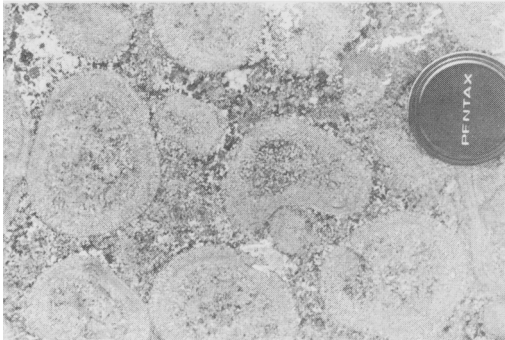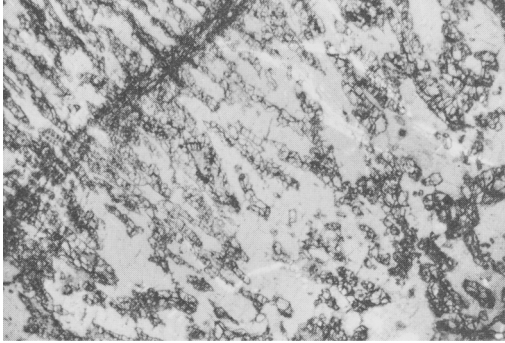
FIGS 5 and 6. FIG. 5 (*top*). Photomicrograph of inner limit of troctolitic shell, showing a gradational boundary into the core gabbro. P.P.L. Width of field 1.5 mm. FIG. 6 (*bottom*). Field photograph showing an orbicule with a deformed troctolitic shell.

FIGS 7 and 8. FIG. 7 (*top*). Photomicrograph showing structure of olivine and plagioclase crystals in the troctolitic shell. Crossed polars, longer side of photograph 1 mm. Note the characteristic 'arrow head' twinning in the plagioclase. FIG. 8 (*bottom*). Photomicrograph of cross-cutting vein at border of troctolitic shell and core gabbro. In the radial shell the vein is filled by orthopyroxene, partly replacing olivine. In the gabbro the vein has a zoned structure with spinel (dark) and magnesian chlorite replacing olivine and pyroxene. P.P.L. Width of field 1 mm.

at present. Numerous xenolithic blocks were caught up in the magma, and some became rounded by assimilation and fracturing.

(*b*) Any pyroxenite left in the future orbicule cores was transformed to amphibolite. Shell layers accumulated outside the amphibolite xenoliths. They may either have done so as a protocrystalline magmatic material before the magma began to rise, or during uprise by rapid crystallization when the magma was strongly oversaturated with olivine and plagioclase.

(*c*) The gabbroic magma, now orbicule-bearing, was introduced at a higher level in the magmatic arc, among pyroclastic rocks and previous hypabyssal intrusions.

(*d*) The core gabbro of the orbicules crystallized before the matrix, at the same time as the radial shell, or a little later. Metamorphism of the core materials began before the matrix had solidified. A variety of orbicule core types was produced (see figure caption).

(*e*) The hydrous matrix solidified, with a variable texture. H_2O escaped from the cores along

fractures, causing metamorphism of pyroxenes to actinolitic amphibole in the outer parts of the core, and of olivine to orthopyroxene in the troctolitic shell.

Some of the cores of the orbicules appear to be fragments of country rocks. The angular shape of some orbicules can be explained by growth of the shells over angular xenolithic fragments. The amphibole aggregated fragments in the cores may be relict fragments of metasomatized ultrabasic rocks, and the presence of magnesian amphibole (Table 2) supports this suggestion. This possibility for the origin of orbicule cores has also been suggested by Leveson (1963) who commented that hornblende might constitute 90% of orbicule cores. Palmer *et al.* (1967) recorded a similar presence of hornblende in Antarctic orbicules, and Perttunen (1983) emphasized the existence of
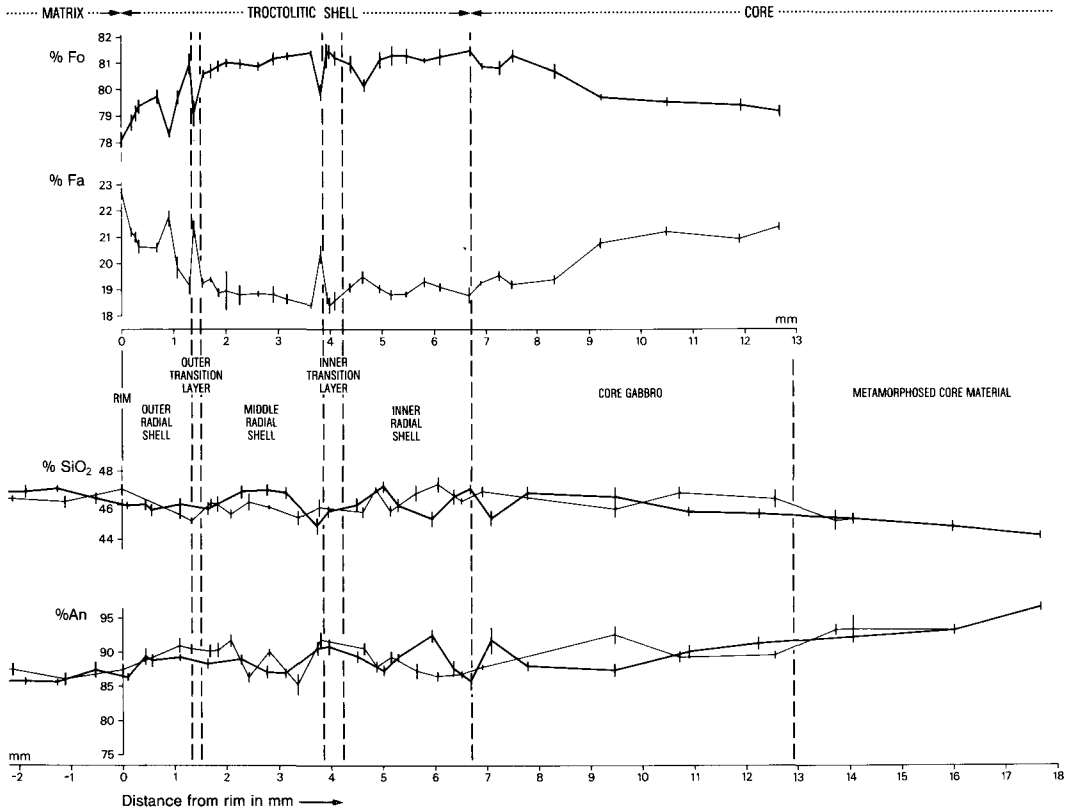
FIG. 9. Variation in olivine and plagioclase composition from matrix (left) into the core (right), including gabbroic and metamorphic parts of core. Vertical bars show 1 sigma variation in count rate for each analysed point. Analyses by wavelength dispersion using Cambridge Instruments Microscan Mark V microprobe at University College, London.

ultramafic cores in orbicules from Kemi, Finland. Keleman and Ghiorso (1986) have put forward the idea that assimilation of ultrabasic materials by magma may be a very significant process in the evolution of igneous rocks above subduction zones. Ultrabasic rocks are present at a lower structural level in the Baskil region. The shapes of the orbicules demonstrate that in some instances the shells overgrew angular solid cores. The gabbroic material of the cores is harder to explain. The deformation of the shell mentioned above suggests that the core gabbro was plastic, if not liquid, after the shells had formed.

The formation of the shell layers is the characteristic event which gave rise to the orbicular structures. It is not possible to tell whether the shells formed round the cores at depth near the ultrabasic country rocks, or during uplift to the present structural level. Alternative hypotheses for the origin of the troctolitic shells are (a) the shells formed as a protocrystalline plastic solid,

as envisaged by Van Diver (1970) and Elliston (1984), which subsequently crystallized as radial intergrowths of olivine and plagioclase or (b) the shells crystallized immediately as radial aggregates of olivine and plagioclase, during rapid crystal growth brought on by release of pressure during the upward movement of the magma (Lofgren and Donaldson, 1975).

(a) Protocrystalline shell growth. The plastic deformation observed in some orbicules supports a hypothesis that the shells developed at supersolidus temperatures as a plastic protocrystalline material, which physically separated the core gabbro from the matrix gabbro. The slight zonation of the olivine crystals is explained as due to diffusive processes occurring in the protocrystalline shell before the crystals formed (McBirney and Noyes, 1979), which was preserved during the later crystallization of the olivine. The radial texture of the shells is regarded as analogous to the

TABLE 3. Microprobe analyses of pyroxenes and amphiboles from the gabbro matrix: (G) magmatic gabbro minerals; (M) secondary metamorphic minerals of matrix.

Pyroxenes

	G	G	G	G
SiO_2	54.82	53.48	53.39	53.94
Al_2O_3	1.48	2.48	1.87	1.59
TiO_2	0.29	0.50	0.21	0.20
Fe_2O_3	0.00	0.34	1.47	0.97
FeO	15.86	14.85	14.35	14.01
MnO	0.43	0.40	0.43	0.37
MgO	22.29	25.60	26.89	27.82
CaO	1.40	1.36	1.03	0.56
Total	96.57	100.00	99.65	99.46

Formulae calculated on the basis of 6 oxygens
(Fe^3 calculated for 4 cations)

Si	2.042	1.929	1.934	1.948
Aliv	0.000	0.071	0.066	0.052
Alvi	0.065	0.035	0.014	0.015
Ti	0.008	0.014	0.006	0.005
Fe3	0.000	0.009	0.040	0.026
Fe2	0.494	0.448	0.435	0.423
Mn	0.014	0.012	0.013	0.011
Mg	1.238	1.430	1.452	1.497
Ca	0.056	0.053	0.040	0.022
En	0.69	0.74	0.75	0.77
Ofs	0.28	0.24	0.23	0.22
Wo	0.03	0.03	0.02	0.01

Amphiboles

	M	M	M	M	M	M	M	G	G	G	G	G
SiO_2	57.40	52.11	50.53	50.87	51.07	48.30	46.17	45.79	45.30	46.47	44.49	44.41
Al_2O_3	1.39	4.57	5.79	6.47	5.65	7.95	11.21	10.41	10.62	12.51	11.41	11.22
TiO_2	0.00	0.14	0.42	0.20	0.34	1.04	0.13	1.07	2.20	0.00	2.35	2.11
Cr_2O_3	0.00	0.00	0.45	0.00	0.45	0.00	0.00	0.18	0.00	0.00	0.00	0.00
Fe_2O_3	7.14	7.27	9.06	10.29	8.32	10.98	12.62	7.72	6.78	10.19	6.27	7.73
FeO	2.57	4.97	3.11	1.19	3.45	0.53	2.71	5.79	6.53	0.00	5.98	3.71
MnO	0.32	0.20	0.23	0.20	0.26	0.26	0.31	0.18	0.26	0.16	0.26	0.00
MgO	19.23	16.44	16.28	17.52	17.03	15.75	13.79	14.01	13.82	16.90	14.39	15.22
CaO	11.71	11.68	11.29	11.61	11.65	10.93	10.99	11.42	11.38	11.67	11.72	11.24
Na_2O	0.00	0.55	0.78	0.83	1.10	1.40	1.46	1.71	1.83	2.00	2.05	2.25
K_2O	0.00	0.00	0.00	0.16	0.15	0.10	0.00	0.26	0.24	0.16	0.29	0.19
Total	99.76	97.93	97.95	99.34	99.47	98.24	99.38	98.54	98.96	100.06	99.21	98.07

Formulae calculated on the basis of 23 oxygens
(Fe^{3+} calculated for 13 cations)

|												
Si	7.815	7.371	7.147	7.060	7.132	6.800	6.520	6.563	6.482	6.422	6.349	6.357
Aliv	0.185	0.629	0.853	0.940	0.868	1.200	1.480	1.437	1.518	1.578	1.651	1.643
Alvi	0.038	0.134	0.113	0.119	0.062	0.119	0.386	0.322	0.273	0.460	0.269	0.250
Ti	0.000	0.015	0.045	0.021	0.036	0.110	0.014	0.115	0.237	0.000	0.252	0.227
Cr	0.000	0.000	0.050	0.000	0.050	0.000	0.000	0.020	0.000	0.000	0.000	0.000
Fe3	0.731	0.774	0.965	1.075	0.874	1.164	1.341	0.833	0.731	1.060	0.673	0.832
Fe2	0.292	0.588	0.368	0.138	0.403	0.062	0.320	0.694	0.781	0.000	0.714	0.444
Mn	0.037	0.024	0.028	0.024	0.031	0.031	0.037	0.022	0.032	0.019	0.031	0.000
Mg	3.902	3.466	3.432	3.624	3.544	3.514	2.902	2.993	2.947	3.481	3.061	3.247
Ca	1.708	1.770	1.711	1.727	1.743	1.649	1.663	1.754	1.745	1.728	1.792	1.724
Na	0.000	0.151	0.214	0.223	0.298	0.382	0.400	0.475	0.508	0.536	0.567	0.624
K	0.000	0.000	0.000	0.028	0.027	0.018	0.000	0.048	0.044	0.028	0.053	0.035
Sum Tet	8.000	8.000	8.000	8.000	8.000	8.000	8.000	8.000	8.000	8.000	8.000	8.000
M1-M3	5.000	5.000	5.000	5.000	5.000	5.000	5.000	5.000	5.000	5.019	5.000	5.000
M4	1.708	1.921	1.925	1.950	2.000	2.000	2.000	2.000	2.000	2.000	2.000	2.000
A	0.000	0.000	0.000	0.000	0.068	0.049	0.063	0.277	0.296	0.292	0.412	0.383

harrisitic textures developed in ultrabasic layered intrusions.

(*b*) *Rapid growth.* During rapid uprise of gabbroic magma, pressure release could cause supercooling below the solidus temperature. The olivine and plagioclase would crystallize rapidly from the supercooled magma, with a radiating skeletal habit. This hypothesis envisages the radial habit of the crystals in the shells as analogous to the radial habits of rapidly cooled crystals in komatiites (Donaldson, 1982), spilitic pillow lavas (Vuagnat, 1946) and comb layering in intrusions (Taubeneck and Poldervaart, 1960; Moore and Lockwood, 1973). The zonation of the olivine would reflect variations in composition at the growing crystal front, implying that growth was sufficiently rapid to outstrip the equilibration of magma composition by diffusion or convection. The 'arrow head' pattern of twinning in the radial plagioclase may support this hypothesis.

It is clear that the orbicule shells acted as a barrier between the gabbro of the core and that

FIG. 10. Cartoon to illustrate the sequence of events during the evolution of the orbicular gabbro (see the text). (*a*) Intrusion of basaltic magma into pyroxenite and amphibolite country-rocks: (1) block rims undergoing transformation from pyroxenite to amphibolite; (2) smaller fragments completely amphibolitized. (*b*) The amphibolitic cores are surrounded by the shell layers. (*c*) The xenolithic magma is intruded at a higher level in the magmatic arc. (*d*) The core gabbro of the orbicules has crystallized. A variety of orbicule core types has arisen: (1) xenolith with core of amphibole aggregate, surrounded by metamorphosed gabbro; (2) xenolith with a metamorphic core surrounded by unmetamorphosed gabbro; (3) xenolith with only a metamorphic core; (4) xenolith with only a gabbro core; (5) complete orbicular structure, as in Fig. 3; (6) shows plastic deformation of radial troctolitic shell, as in Fig. 6. In this case there is no unmetamorphosed gabbro in the core at present, but the core gabbro was plastic during the deformation. (*e*) Hydrous gabbro matrix solidifies, with variable texture. H_2O escapes from the cores along fractures: (1) troctolitic outer shell with radial texture; (2) gabbroic layer within core; (3) metamorphic layer within the core; (4) inner core, amphibole aggregate; (5) fracture filled with orthopyroxene.
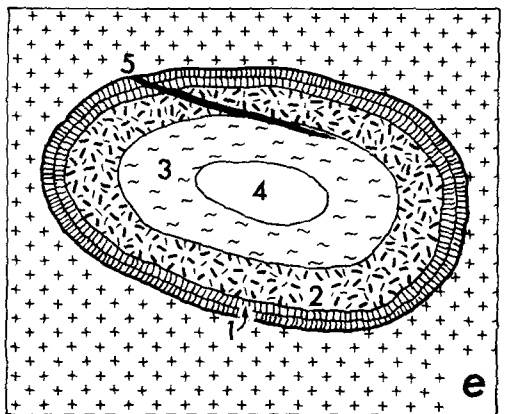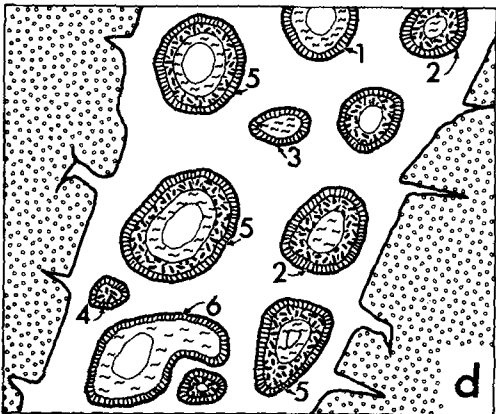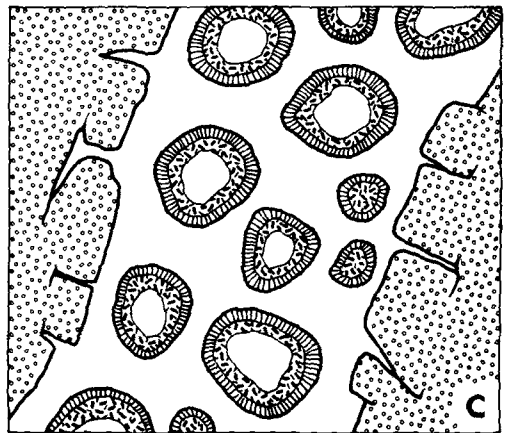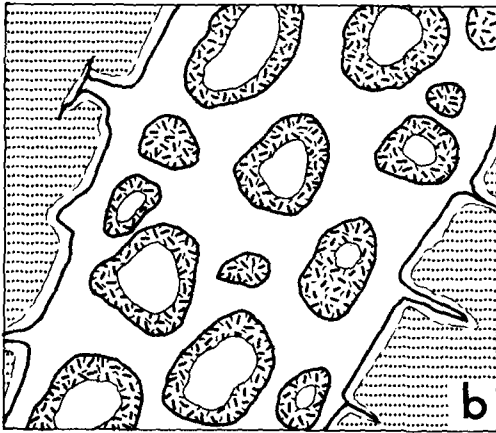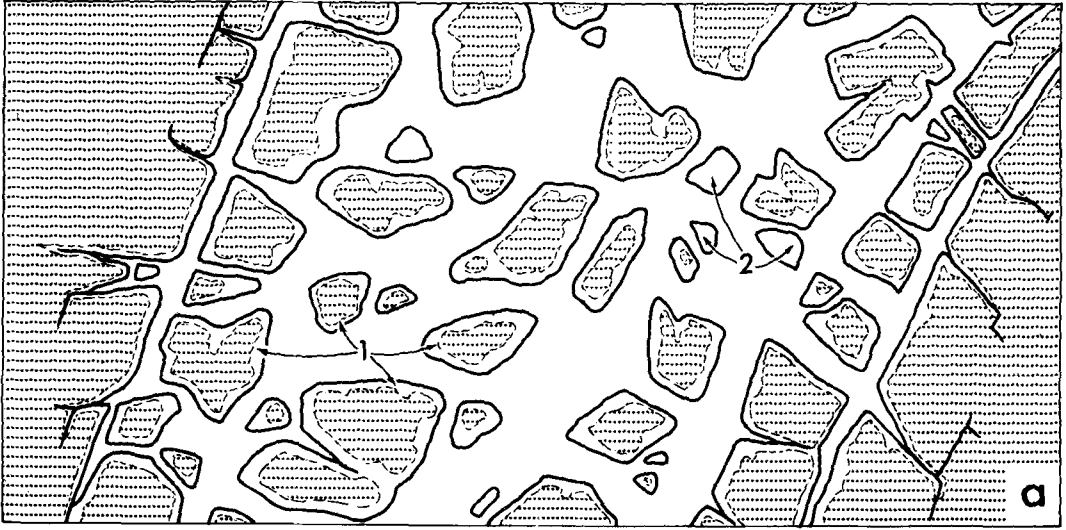
of the matrix (Table 1). The compositions of the olivine and plagioclase in the inner part of the radial shell are very close to those in the core gabbro (Fig. 9), suggesting that the last stage of crystallization of the troctolitic shell passed continuously into the crystallization of the core gabbro. The magnesian composition of the radial olivine, the Ca-rich composition of the radial plagioclase, and the absence of pyroxene in the radial shell all suggest that the shell began to crystallize a little before the core gabbro.

The metamorphism of all the parts of the orbicular gabbro, and the presence of magmatic hornblende in the core and matrix gabbros indicates that the magma was unusually hydrous. The anhydrous primary mineral assemblages in the troctolitic shells may indicate that these crystallized while the magma was still undersaturated with H_2O (Maggetti et al., 1978), while the core and matrix gabbros crystallized at slightly lower temperatures, when the magma had become saturated. The increased abundance of metamorphism in the cores, and the metamorphosed fractures running out of the core interiors through the radial shell, indicate that H_2O was particularly concentrated in the cores. Some of this H_2O could have originated by the dehydration of amphiboles in the amphibole aggregate core material.

Metamorphism is most widespread in the cores of the orbicules, occurs in the troctolitic shells only along the orthopyroxene filled fractures, and is rare in the matrix gabbro. It is considered to be the product of excess H_2O produced in the cores during crystallization of the hydrous core gabbro, which then escaped through fractures in the already crystallized troctolitic shells. Olivine was transformed to orthopyroxene by SiO_2 in solution in the H_2O, and olivine + plagioclase was locally altered to spinel + actinolite.

This study is not conclusive in presenting a single theory for the mode of origin of the orbicules, and it is clear that further research is needed. The mode of origin of the radial troctolitic shells is crucial to the development of orbicules, and this remains unresolved.

Acknowledgements

References

Augustithis, S. S. (1982) Atlas of the sphaeroidal textures and structures and their genetic significance. Athens: Theophrastus Publications.

Barrière, M. (1972) Le gabbro orbiculaire des Alharesses (massif de Neauvielle, Pyrénées françaises). Bull. Soc. Franc. Minéral. Crist. 95, 495–506.

Campbell, I. (1906) Orbicular gabbro from Black Butte, Los Angeles County, California. Am. Mineral. 27, 218–9.

Carstens, H. (1957) On the orbicular structure in the norite of Pamsaas, Norway. Norsk Geol. Tidsskr. 37, 279–80.

Coleman, R. G. (1977) Ophiolites: ancient oceanic lithosphere. New York: Springer.

Donaldson, H. C. (1982) Spinifex-textured komatiites: a review of textures, compositions and layering. In Komatiites (Arndt, N. T. and Nisbet, E. G., eds.). London: Allen & Unwin, 213–44.

Elliston, J. N. (1984) Orbicules: an indication of the crystallization of hydrosilicates, I. Earth Sci. Rev. 20, 265–344.

Eskola, P. (1938) On the esboitic crystallisation of orbicular rocks. J. Geol. 46, 448–85.

Frosterus, B. (1892) Tschermak's Mineral. Petrog. Mitt. 13, 177–210.

——(1896) Bull. Comm. géol. Finlande 4, 1–38.

Kelemen, P. B. and Ghiorso, M. S. (1986) Assimilation of peridotite in zoned calc–alkaline plutonic complexes: evidence from the Big Jim complex, Washington Cascades. Contrib. Mineral. Petrol. 94, 12–28.

Lawson, A. C. (1902) On an orbicular gabbro from San Diego County, California (abstract). Science 15, 415.

Lee, C. A. and Sharpe, M. R. (1979) Sphaeroidal pyroxenite aggregates in the Bushveldt Complex. A special case of silicate liquid immiscibility. Earth Plant. Sci. Lett. 44, 295–310.

Leveson, D. J. (1963) Orbicular rocks of the Lonesome Mountain area, Beartooth Mountains, Montana and Wyoming. Geol. Soc. Am. Bull. 74, 1015–40.

——(1966) Orbicular rocks: a review. Ibid. 77, 409–26.

Lofgren, G. E. and Donaldson, C. H. (1975) Curved and branching crystals and differentiation in comb-layered rocks. Contrib. Mineral. Petrol. 49, 309–19.

McBirney, A. R. and Noyes, R. M. (1979) Crystallisation and layering of the Skaergaard Intrusion. J. Petrol. 20, 487–554.

Maggetti, M., van Diver, B. B., Galetti, G. and Sommerauer, J. (1978) PT-conditions of orbicular gabbro from Reichenbach, West Germany. Neues Jahrb. Mineral. Abh. 134, 52–75.

Maisonneuve, J. (1960) Etude géologique sur la Sud de la Corse. Bull. Service cart. géol. France 57, No. 260, 41–161.

Mason, R. (1978) Petrology of the Metamorphic Rocks. London: Allen & Unwin.

Merriam, R. (1958) Orbicular gabbro near Pine Valley, California. Southern California Acad. Sci. Bull. 57, 24–33.

Moore, J. G. and Lockwood, J. P. (1973) Origin of

comb layering and orbicular structure, Sierra Nevada batholith, California. *Geol. Soc. Am. Bull.* **84**, 1–20.

Palmer, D. F., Bradley, J. and Prebble, W. M. (1967) Orbicular granodiorite from Taylor Valley, South Victoria Land, Antarctica. Ibid. **78**, 1423–8.

Perttunen, V. (1983) Orbicular quartz diorite in Kemi, NW Finland. *Bull. Geol. Soc. Finland* **55**, part 2, 51–6.

Satterly, J. (1940) An orbicular gabbro from Tremeer Lake, Kenora district, Ontario. *Toronto Univ. Studies Geol. Ser.* **44**, 75–82.

Schaller, W. T. (1911) Orbicular gabbro from Pala San Diego County, California. *U.S. Geol. Surv. Bull.* **490**, 58–9.

Sederholm, J. J. (1928) On orbicular granites, spotted and nodular granites etc. and on the rapakivi texture. *Bull. Comm. Geol. Finl.* **83**, 1–105.

Simonen, A. (1940) Orbicular rocks in Kemijarvi and Esbo. Ibid. **128**, 107–40.

——(1966) Orbicular rock in Kuru, Finalnd. *Comptes Rendus Soc. Geol. Finl.* **38**, 93–107.

Taubeneck, W. H. and Poldervaart, A. (1960) Geology of the Elkhorn Mountains, northeastern Oregon: Part 2. Willow Lake Intrusion. *Geol. Soc. Amer. Bull.* **71**, 1295–322.

Van Diver, B. B. (1970) Origin of biotite orbicules in 'Bullseye granite' of Craftsbury, Vermont. *Am. J. Sci.* **268**, 322–40.

——and Maggetti, M. (1975) Orbicular gabbro from Reichenbach in the Bergstrasser Odenwald, Germany. *Neues Jahrb. Mineral. Abh.* **125**, 1–26.

Vuagnat, M. (1946) Sur quelques diabases suisses. Contribution à l'étude du problème des spilites et des pillow lavas. *Mineral. Petrogr. Mitt.* **26**, 116–228.

Watson, T. L. (1904) Orbicular gabbro-diorite from Davie County, North Carolina. *J. Colloid. Sci.* **5**, 85–97.

Yazgan, E. (1983) Geodynamic evolution of the Eastern Taurus region. In *Geology of the Taurus belt* (Tekeli, O. and Göncüoğlu, M. C., eds.). International Symposium 26–29 September, Ankara, Turkey, 199–208.

——Michard, A., Whitechurch, H. and Montigny, R. (1983) Le Taurus de Malatya (Turquie orientale), élément de la suture sud-téthysienne. *Bull. Soc. géol. France* **25**, 59–69.